

UNIVERSIDADE FEDERAL DE SANTA CATARINA
PROGRAMA DE PÓS-GRADUAÇÃO EM ENGENHARIA MECÂNICA

MODELO DE VIBRAÇÕES DE VIGAS DE REFORÇO
UTILIZADAS EM PLATAFORMAS OFSHORE

Tese submetida à

UNIVERSIDADE FEDERAL DE SANTA CATARINA

para a obtenção do grau de

DOUTOR EM ENGENHARIA MECÂNICA

ALEXANDRE AUGUSTO PESCADOR SARDÁ

Florianópolis, maio de 2004.

UNIVERSIDADE FEDERAL DE SANTA CATARINA
PROGRAMA DE PÓS-GRADUAÇÃO EM
ENGENHARIA MECÂNICA

**VIBRATION MODELS FOR REINFORCING BEAMS USED IN OFFSHORE
PLATE STRUCTURES**

ALEXANDRE AUGUSTO PESCADOR SARDÁ

Esta tese foi julgada adequada para a obtenção do título de

DOUTOR EM ENGENHARIA

ESPECIALIDADE ENGENHARIA MECÂNICA

sendo aprovada em sua forma final.

Prof. José Antônio Bellini da Cunha Neto, Dr.

Arcanjo Lenzi, Ph.D. – Orientador

Joseph Cuschieri, Ph.D. – Co-orientador

BANCA EXAMINADORA

Prof. Arcanjo Lenzi, Ph.D. – Presidente

Prof. Moyses Zindeluck, D.Sc.

Prof. Valder Steffen Junior, Dr.

Prof. Roberto Jordan, Dr. Eng.

Prof. Marcelo Krajnc Alves, Ph.D.

To
My wife and my family

ACKNOWLEDGMENTS.

First, I would like to thank Professor Arcanjo Lenzi for giving me the opportunity to begin the studies in the vibration and acoustics area and, also, for his friendship.

I would also like to thank Dr. Joseph Cuschieri for accepting me at Florida Atlantic University as a visitor student and giving me all the support for the one year I spent there.

I would like to thank the LVA colleagues and friends , Paulo Boni, Vitor, João, Fábio, Marcão, Wiliam, Humberto and Marcelo.

I would like to fully thank my family and my wife Heloisa.

Finally, I would like to thank the agencies CNPq and Capes for the financial support and the Federal University of Santa Catarina (UFSC) and Florida Atlantic University (F.A.U.) for accepted me as a doctoral student.

TABLE OF CONTENTS

LIST OF SYMBOLS.....	vii
LIST OF FIGURES.....	x
ABSTRACT.....	xvi
RESUMO.....	xvii
CHAPTER 1 OVERVIEW OF STRUCTURAL ACOUSTICS.....	1
1.1 INTRODUCTION.....	1
1.2 LITERATURE REVIEW.....	3
CHAPTER 2 BASIC CONCEPTS.....	22
2.1 FLEXURAL WAVES IN THIN PLATES.....	23
2.2 IN-PLANE VIBRATIONS FOR THIN PLATES.....	28
2.3 BOUNDARY CONDITIONS FOR THIN PLATES.....	31
CHAPTER 3 ANALYTICAL MODELS FOR BEAMS.....	34
3.1 IN-PLANE WAVE SOLUTIONS.....	35
3.2 BENDING WAVES SOLUTION.....	37
3.3 ANALYTICAL MODEL FOR TWO CONNECTED L-SHAPED PLATES.....	38
3.4 ANALYTICAL MODEL FOR THREE CONNECTED PLATES IN A T CONFIGURATION.....	47
CHAPTER 4 IMAGE METHOD.....	54
4.1 DRIVING-POINT IMPEDANCE OF HOMOGENEOUS PLATES IN FLEXURE.....	55
4.2 IMAGE METHOD APPLIED TO RECTANGULAR PLATES.....	60
4.3 SEMI-INFINITE PLATE.....	62
4.4 APPLICATION OF THE IMAGE METHOD TO A SIMPLY SUPPORTED RECTANGULAR PLATE EXCITED BY A TRANSVERSAL FORCE.....	65
4.5 SIMPLY SUPPORTED RECTANGULAR PLATE EXCITED BY A MOMENT.....	72
4.6 CORRECTION FUNCTIONS FOR A SEMI-INFINITE PLATE.....	77
4.6.1 Fundamental solution for a simply supported and a roller boundary condition.....	77
4.6.2 Obtention of fundamental solution for clamped edge via	

correction to simply supported edge.....	79
4.6.3 Obtention of fundamental solution for free edge via correction to simply supported edge.....	84
4.6.4 Correction factor – Analysis of the influence of the integral tolerance on the clamped edge correction.....	88
4.6.5 Correction factor – Application to a semi-infinite plate.....	90
4.7 VIBRATION OF A THREE DIMENSIONAL PARALLELEPIPED.....	93
CHAPTER 5 CONNECTED PLATES WITH A BEAM ON THE JOINT LINE.....	101
5.1 ANALYTICAL MODEL FOR TWO CONNECTED PLATES WITH AN L BEAM ON THE JOINT LINE.....	102
5.2 TWO CONNECTED PLATES WITH AN L BEAM ON THE JOINT LINE – INPUT MOBILITY.....	114
5.3 VIBRATION ANALYSIS FOR TWO CONNECTED PLATES WITH AN L BEAM ON THE JOINT LINE.....	120
5.4 POWER FLOW BETWEEN PLATE REINFORCED BEAM.....	124
WITH AN L BEAM ON THE JOINT LINE.....	124
CHAPTER 6 CONCLUSIONS.....	127
REFERENCES.....	130
APPENDIX A DERIVATION OF THE EXPRESSIONS FOR θ , Q_y , AND M	137

LIST OF SYMBOLS

A_1 to A_{32}	Constants to be determined
A to Q	Constants to be determined
c_l	Longitudinal wave velocity
c_s	Shear wave velocity
c	Sound speed in air
D	Plate's bending stiffness
E	Young modulus of the plate
G	Shear stiffness
G_∞	Green's function or fundamental solution to the deflection of an infinite plate
G_s	Fundamental solution to the deflection of a simple supported plate
G_r	Fundamental solution to the deflection of a roller boundary plate
G_f	Fundamental solution to the deflection of a free edge boundary plate
h	plate's thickness
$H_0^{(1)}$	Hankel function of zero order and first kind
$H_0^{(2)}$	Hankel function of zero order and second kind
k	wavenumber
k_l	Longitudinal wavenumber
k_s	Shear wavenumber
m'	Mass per unity area of the plate
M_x	Bending moment per unit length
M_y	Bending moment per unit length
M_{yx}	Torsional moment per unit length

N_x	Force per unit length
N_y	Force per unit length
N_{xy}	Force per unit length
q	Externally applied load
Q_x	Shear force per unit length
Q_y	Shear force per unit length
t	Time
u	Displacement on the y direction
U	Fundamental solution to the deflection of an infinite plate
v	Displacement on the y direction
$\langle \bar{v}^2 \rangle$	Average mean-square velocity
V_x	Force per unit length
w	Transversal displacement on the z direction
ρ	Density
η	Loss factor
ϵ_x	Normal strain on the x direction
ϵ_y	Normal strain on the y direction
ϵ_z	Normal strain on the z direction
γ_{xy}	Shear strain in the plane
λ	First Lamé constant
σ_x	Normal stress on the x direction
σ_y	Normal stress on the y direction
σ_z	Normal stress on the z direction
τ_{xy}	Shear stress on the xy plane
ν	Poisson ratio
ω	Angular frequency
ϕ_d	Potential functions for longitudinal rotation
ψ_s	Potential functions for shear rotation

NOTATIONS

∇^2 Laplacian

* Complex conjugate

j $\sqrt{-1}$.

Re{ } Real part of a complex number

Im{ } Imaginary part of a complex number

LIST OF FIGURES AND TABLES

CHAPTER 1 OVERVIEW OF STRUCTURAL ACOUSTICS

Figura 1.1: a) typical wall of an offshore platform.....	2
b) typical floor of an offshore platform.....	2
Figure 1.2 – Boundary condition used – two clamped nodes.....	16
Figura 1.3 – View of the beam reinforced model plate Finite Element Mesh.....	16
Figura 1.4 – Detailed view of the beam reinforced model plate Finite Element Mesh.....	17
Figure 1.5 – Power flow between subsystems 1 and 2. Comparison between plate element and beam element, inverted T beam, 5 cm height; base 2.5 cm; thickness 0.25 cm.....	18
Figure 1.6 – Power flow between subsystems 1 and 2. Comparison between plate element and beam element, inverted T beam, 20 cm height; base 10.0 cm; thickness 1.0 cm.....	18
Figure 1.7 – Coupling loss factor for subsystem 1 and 2. Comparison between plate element and beam element, inverted T beam, 5 cm height; base 2.5 cm; thickness 0.25 cm.....	19
Figure 1.8 – Coupling loss factor for subsystems 1 and 2. Comparison between plate element and beam element, T inverted beam, 20 cm height; base 10.0 cm; thickness 1.0 cm.....	19

CHAPTER 2 BASIC CONCEPTS

Figure 2.1 – (a) Thin plate element.....	23
Figure 2.2 – (a) differential element of plate. (b) side view of the element during	

bending. (c) top view of the lamina showing shear defformation.....	25
Figure 2.3 – Thin plate submitted to in-plane loads.....	28
Figure 2.4 – Steps in the development of the free edge boundary condition for a plate.....	32

CHAPTER 3 ANALYTICAL MODELS FOR BEAMS

Figure 3.1 – Two L connected bi-supported plates.....	38
Figure 3.2 – Continuity condition at the junction of the plates.....	39
Figure 3.3 – Points of response on each plate.....	44
Figure 3.4 – Transversal displacement w on plate 1. Comparison between the analytical model and the Finite Element Model for n varying from 1 to 2.....	44
Figure 3.5 – In-plane displacement u for plate 1. Comparison between the analytical model and the Finite Element Model for n varying from 1 to 2.....	45
Figura 3.6 – In-plane displacement v for plate 1. Comparison between the analytical model and the Finite Element Model for n varying from 1 to 2.....	45
Figure 3.7 - Transversal displacement w on plate 2. Comparison between the analytical model and the Finite Element Model for n varying from 1 to 2.....	46
Figure 3.8 – In-plane displacement u for plate 2. Comparison between the analytical model and the Finite Element Model for n varying from 1 to 2.....	46
Figura 3.9 – In-plane displacement v for plate 2. Comparison between the analytical model and the Finite Element Model for n varying from 1 to 2.....	47
Figure 3.10 – Three coupled plates in a T configuration.....	48
Figura 3.11 – Loads acting on each plate.....	49
Figure 3.12 - Transversal displacement w on plate 1. Comparison between the analytical model and the Finite Element Model for n varying from 1 to 2.....	52
Figure 3.13 - Transversal displacement w on plate 2. Comparison between the analytical model and the Finite Element Model for n varying from 1 to 2.....	52

CHAPTER 4 IMAGE METHOD

Figure 4.1 - Infinite plate submitted to an applied concentrated force.....	56
Figure 4.2 – Plate representation.....	61

Figure 4.3 – Imaging for semi-infinite plate.....	63
Figure 4.4 – Infinite plate with positive (+) and negative (-) sources equivalent to simply supported plate with edges E_1 , E_2 , E_3 and E_4 excited at (x_s, y_s)	66
Figure 4.5 – Simple supported plate, $L_x=L_y=1.0$ m, $h=0.002$ m, $x_s = y_s=0.5$ m, $x = y =0.25$ m, $E=72 \cdot 10^9$ N/m ² , $\rho=2710$ kg/m ³ , $\nu=0.27$, $\eta=0.03$. Displacement as a function of number of images used in each direction ($n=15$).....	66
Figure 4.6 – Simple supported plate, $L_x=L_y=1.0$ m, $h=0.002$ m, $x_s = y_s=0.5$ m, $x = y =0.25$ m, $E=72 \cdot 10^9$ N/m ² , $\rho=2710$ kg/m ³ , $\nu=0.27$, $\eta=0.03$. Displacement as a function of number of images used in each direction ($n=51$).....	67
Figure 4.7 – Simple supported plate, $L_x=L_y=1.0$ m, $h=0.002$ m, $x_s = y_s=0.5$ m, $x = y =0.25$ m, $E=72 \cdot 10^9$ N/m ² , $\rho=2710$ kg/m ³ , $\nu=0.27$, $\eta=0.03$. Displacement as a function of number of images used in each direction ($n=151$).....	67
Figure 4.8 – Simple supported plate, $L_x=L_y=5.0$ m, $h=0.002$ m, $x_s = y_s=2.0$ m, $x = y =1.0$ m, $E=72 \cdot 10^9$ N/m ² , $\rho=2710$ kg/m ³ , $\nu=0.27$, $\eta=0.03$. Displacement as a function of number of images used in each direction ($n=5$).....	68
Figure 4.9 – Simple supported plate, $L_x=L_y=5.0$ m, $h=0.002$ m, $x_s = y_s=2.0$ m, $x = y =1.0$ m, $E=72 \cdot 10^9$ N/m ² , $\rho=2710$ kg/m ³ , $\nu=0.27$, $\eta=0.03$. Displacement as a function of number of Images used in each direction ($n=15$).....	69
Figure 4.10 – Simple supported plate, $L_x=L_y=5.0$ m, $h=0.002$ m, $x_s = y_s=2.0$ m, $x = y =1.0$ m, $E=72 \cdot 10^9$ N/m ² , $\rho=2710$ kg/m ³ , $\nu=0.27$, $\eta=0.03$. Displacement as a function of number of Images used in each direction ($n=51$).....	69
Figure 4.11 – Simple supported plate, $L_x=L_y=5.0$ m, $h=0.002$ m, $x_s = y_s=2.0$ m, $x = y =1.0$ m, $E=72 \cdot 10^9$ N/m ² , $\rho=2710$ kg/m ³ , $\nu=0.27$, $\eta=0.01$. Displacement as a function of damping ($\eta = 0.01$).....	70
Figure 4.12 – Simple supported plate, $L_x=L_y=5.0$ m, $h=0.002$ m, $x_s = y_s=2.0$ m,	

	$x = y = 1.0 \text{ m}$, $E = 72 \cdot 10^9 \text{ N/m}^2$, $\rho = 2710 \text{ kg/m}^3$, $\nu = 0.27$, $\eta = 0.03$.	
	Displacement as a function of damping ($\eta = 0.03$).....	71
Figure 4.13 – Simple supported plate, $L_x=L_y=5.0 \text{ m}$, $h=0.002 \text{ m}$, $x_s = y_s=2.0 \text{ m}$,	$x = y = 1.0 \text{ m}$, $E = 72 \cdot 10^9 \text{ N/m}^2$, $\rho = 2710 \text{ kg/m}^3$, $\nu = 0.27$, $\eta = 0.1$.	
	Displacement as a function of damping ($\eta = 0.1$).....	71
Figure 4.14 – Simple supported rectangular plate with applied concentrated moment.....		73
Figure 4.15 – Infinite plate with positive (+) and negative (-) sources equivalent to simply supported plate with edges E_1 , E_2 , E_3 and E_4 excited by a concentrated moment at (x_s, y_s)		73
Figure 4.16 – Simple supported plate, $L_x=L_y=5.0 \text{ m}$, $h=2 \text{ mm}$, $x_s = y_s=2.0 \text{ m}$,	$x = y = 1.0 \text{ m}$, $E = 72 \cdot 10^9 \text{ N/m}^2$, $\rho = 2710 \text{ kg/m}^3$, $\nu = 0.27$, $\eta = 0.03$.	
	Displacement. Number of images in each direction: 5.....	74
Figure 4.17– Simple supported plate, $L_x=L_y=5.0 \text{ m}$, $h=2 \text{ mm}$, $x_s = y_s=2.0 \text{ m}$,	$x = y = 1.0 \text{ m}$, $E = 72 \cdot 10^9 \text{ N/m}^2$, $\rho = 2710 \text{ kg/m}^3$, $\nu = 0.27$, $\eta = 0.03$.	
	Displacement. Number of images in each direction: 15.....	74
Figure 4.18 – Simple supported plate, $L_x=L_y=5.0 \text{ m}$, $h=2 \text{ mm}$, $x_s = y_s=2.0 \text{ m}$,	$x = y = 1.0 \text{ m}$, $E = 72 \cdot 10^9 \text{ N/m}^2$, $\rho = 2710 \text{ kg/m}^3$, $\nu = 0.27$, $\eta = 0.03$.	
	Angular displacement. Number of images in each direction: 5.....	75
Figure 4.19 – Simple supported plate, $L_x=L_y=5.0 \text{ m}$, $h=2 \text{ mm}$, $x_s = y_s=2.0 \text{ m}$,	$x = y = 1.0 \text{ m}$, $E = 72 \cdot 10^9 \text{ N/m}^2$, $\rho = 2710 \text{ kg/m}^3$, $\nu = 0.27$, $\eta = 0.03$.	
	Angular displacement. Number of images in each direction: 15.....	75
Figure 4.20 – Semi infinite plate with an applied concentrated force.....		78
Figure 4.21 – Moment of a semi-infinite plate with clamped edge correction, 1.0 m by 1.0 m, $h = 2.0 \text{ mm}$, $F=1$ at $x = 0.5 \text{ m}$, $y = 0.5 \text{ m}$, 2.0 frequency = 50 Hz, $\eta = 0.1$		81
Figure 4.22 – Moment of a semi-infinite plate with clamped edge correction, 1.0 m by 1.0 m, $h = 2.0 \text{ mm}$, $F=1$ at $x = 0.5 \text{ m}$, $y = 0.5 \text{ m}$, frequency = 500 Hz, $\eta=0.1$		81
Figure 4.23 – Response of a semi-infinite plate, 5.0 m by 1.0 m, $h = 2.0 \text{ mm}$, $F=1$ at $x = 2.5 \text{ m}$, $y = 1.0 \text{ m}$, with simple supported edge (frequency = 10 Hz).($\eta = 0.1$).....		82
Figure 4.24 – Clamped correction applied to a semi-infinite plate, 5.0 m by 1.0 m,		

$h = 2.0$ mm, $F=1$ at $x = 2.5$ m, $y = 1.0$ m (frequency = 10 Hz). ($\eta = 0.1$).....	83
Figure 4.25 – Response of a semi-infinite plate, 5.0 m by 1.0 m, $h = 2.0$ mm, $F=1$ at $x = 2.5$ m, $y = 1.0$ m, with clamped correction applied to a simple supported edge (frequency = 10 Hz).($\eta = 0.1$).....	83
Figure 4.26 – Response of a semi-infinite plate, 5.0 m by 1.0 m, $h = 2.0$ mm, $F=1$ at $x = 2.5$ m, $y = 1.0$ m, with clamped correction applied to a simple supported edge (frequency = 10 Hz).($\eta = 0.1$).....	84
Figure 4.27 – Variation of the integrand with the component of the wavenumber k_x	86
Figure 4.28 – Response of a semi-infinite plate, 5.0 m by 1.0 m, $h = 2.0$ mm, $F=1$ at $x = 2.5$ m, $y = 1.0$ m, with free edge correction applied to a simple supported edge (frequency = 10 Hz).($\eta = 0.1$).....	87
Figure 4.29 – Free edge correction applied to a semi-infinite plate, 5.0 m by 1.0 m, $h = 2.0$ mm, $F=1$ at $x = 2.5$ m, $y = 1.0$ m (frequency = 10 Hz). ($\eta = 0.1$) (corrected δ).....	87
Figure 4.30 – Correction to a semi-infinite plate with a clamped edge, $h = 2.0$ mm, $F=1$ at $x = 0$ m, $y = 1.5$ m, $x_s = 0$ m, $y_s = 0.5$ m .($\eta = 0.05$). Variation with the tolerance of the integral.....	88
Figure 4.31 – Correction to a semi-infinite plate with a clamped edge, $h = 2.0$ mm, $F=1$ at $x = 0$ m, $y = 5.5$ m, $x_s = 0$ m, $y_s = 0.5$ m .($\eta = 0.05$) Variation with the tolerance of the integral.....	89
Figure 4.32 – Correction to a semi-infinite plate with a clamped edge, $h = 2.0$ mm, $F=1$ at $x = 0$ m, $y = 1.5$ m, $x_s = 0$ m, $y_s = 0.5$ m .($\eta = 0.05$) Variation of the correction factor with the wave number integration.....	90
Figure 4.33 – Finite Element Method used.....	91
Figure 4.34 – Response point $x = 0.7$ m; $y = 0.2$ m. Semi infinite plate with clamped edges..	92
Figure 4.35 – Response point $x = 0.7$ m; $y = 0.7$ m. Semi infinite plate with clamped edges..	92
Figure 4.36 – Parallelepiped configuration.....	94
Figure 4.37 – Results of the parallelepiped results compared with the Finite Element Method.....	100

CHAPTER 5 CONNECTED PLATES WITH A BEAM ON THE JOINT LINE

Figure 5.1 – Two connected bi-supported plates, with an L beam, modeled as plate elements, on the joint line.....	102
Figure 5.2 – Continuity conditions at the plate joint line.....	104
Figure 5.3 – Transversal displacement w on plate 1. Comparison between the analytical model and the Finite Element Model for n equal to 1 and 2.....	111
Figure 5.4 – In-plane displacement u on plate 1. Comparison between the analytical model and the Finite Element Model for n equal to 1 and 2.....	112
Figure 5.5– In-plane displacement v on plate 1. Comparison between the analytical model and the Finite Element Model for n equal to 1 and 2.....	112
Figure 5.6 - Transversal displacement w on plate 4. Comparison between the analytical model and the Finite Element Model for n equal to 1 and 2.....	113
Figure 5.7– In-plane and out-of-plane internal loading acting on a plate.....	115
Figure 5.8– Internal forces and velocity representation on the joint line of two systems, with an external excitation at point 1.....	115
Figure 5.9 - Transversal displacement w on plate 4. Comparison between the analytical model and the Finite Element Model for n equal to 1 and 2.....	121
Figure 5.10 – Modes for a beam reinforced plate.....	124
Figure 5.11 – Power flow from plate 1 to plate 2.....	126

APPENDIX A DERIVATION OF THE EXPRESSIONS FOR θ , Q_y , AND M

Figure A.1 – Imaging for semi-infinite plate.....	137
---	-----

RESUMO

Placas reforçadas por vigas são os principais componentes de estruturas de plataformas offshore, usadas na prospecção e produção de petróleo. As vibrações geradas pelas máquinas propagam-se através da estrutura gerando altos níveis de ruído nos alojamentos. Para determinar com precisão o fluxo de potência através de placas reforçadas por vigas, um modelo que inclua o efeito das ressonâncias próprias da alma e aba da viga e as ondas no plano deve ser considerado, sendo o efeito das ondas no plano importante principalmente nas altas frequências.

Este trabalho apresenta um modelo para determinar a resposta de placas reforçadas por vigas utilizando uma abordagem analítica. Os modelos incluem vigas L e T e uma placa reforçada por uma viga L submetida a um carregamento distribuído. Este modelo pode ser usado para a determinação dos fatores de acoplamento de estruturas a serem utilizadas em uma análise de Análise Estatística Energética (SEA).

Este método é útil devido ao baixo tempo de processamento comparado aos outros métodos existentes e a precisão é consideravelmente boa especialmente nas altas frequências. Os resultados obtidos são validados comparando-se com o Método de Elementos Finitos.

Outros métodos para a determinação da mobilidade de estruturas tipo placa reforçada por vigas também são apresentados neste trabalho. Um destes métodos é o Método de Imagens, que envolve a distribuição de fontes e imagens de vibrações de forma que obedeça as condições de contorno da estrutura. Este método é aplicável principalmente para estruturas de grandes dimensões e alto amortecimento estrutural.

ABSTRACT

Beam reinforced plates are the main components of offshore structures, used in oil exploration and production. The vibrations generated by machines propagate through the structure and generate usually a high noise level at the accommodation areas. To determine with accuracy the power flow through the plate reinforced by beams, a model that includes the effect of the web and flange resonances in the beam and the in-plane waves is necessary, since in-plane waves are of considerable importance at high frequencies.

This work presents a model to determine the response of beam reinforced plates using an analytical approach. The model includes L and T shaped beams and an L beam reinforced plate submitted to a distributed load. This model can be used to calculate coupling loss factors in reinforced structures to be used in Statistical Energy Analysis.

This method is useful since the processing time is low compared with other methods and the accuracy is good at high frequencies. The results are compared and validated with the Finite Element Method.

Other methods for determining the mobility of plates are also presented. One method is the Image Method, which involves the correct placing of sources and images of vibrations on a plate to obtain the final response satisfying the boundary conditions. This method applies to large structures and high structural damping.

CHAPTER 1

OVERVIEW OF STRUCTURAL ACOUSTICS

1.1 INTRODUCTION

Beam reinforced plates are the main components of structures such as those offshore platforms used in oil prospecting and production. Vibrations generated by machinery on these platforms propagate through the structure and can generate high noise levels in the accommodation areas.

The oil platform structure is composed of beams and plates, as shown in Figures 1.1a and 1.1b. Beams are used to support machines and equipment, and are organized in a “grill” arrangement. Their dimensions range from 2 cm to 20 cm wide, up to 50 cm high, and 5.0 m long. The thickness of the plates ranges from 5 mm to 10 mm.

To determine the power flow and the vibratory energy of such structural components, a knowledge of the mean square velocity $\langle v^2 \rangle$ is valuable. One way of solving this problem is using the Finite Element Method (FEM). The disadvantage of using FEM is the limitation regarding the processing time. At high frequencies, the wavelength becomes smaller,

increasing the number of elements necessary for a correct representation of the model. This method becomes excessively expensive for larger, more complex structures.

In these kinds of structures, models that include the effects of web and flange resonances in the beam and in-plane waves in all the structural components are necessary, since both of these are important, particularly when considering high frequencies analyses of such structures. This work presents a model to determine the response of beam reinforced plates using both an analytical and a direct image method to obtain the component mobility functions for arbitrary boundary conditions. This approach is very efficient computationally and can generate accurate results up to relatively high frequencies.



a)



b)

Figure 1.1: a) typical wall of an offshore platform.

b) typical floor of an offshore platform.

1.2 LITERATURE REVIEW

The vibration analysis of plate like structures can be made using Statistical Energy Analysis (SEA). According to Lyon [1], SEA was created as a methodology for approaching the vibration and acoustics problems using both analytical and experimental methods. The main variable of this method is the energy and it can be applied to structural and acoustics systems. This method is useful in high frequency analysis, where the modal density is usually high, particularly for 3-dimensional acoustical subsystems. However, the application of SEA demands the knowledge of parameters such as the coupling loss factors and the radiation efficiency. Among the parameters used in this methodology, the coupling loss factor requires careful attention when applied to this type of structure due to the great influence which the beams have on the power flow between plates.

The statistical energy analysis (SEA) method was first applied to the structural vibration problem as an extension of the room acoustics approach in acoustical engineering [2]. Developed by Lyon [1] and associates, the method considers the linear responses of multimodal structures and the resulting energy flow between the modes of two or more sets of substructures. The modes of a substructure are called a subsystem.

According to Lenzi [3], Statistical Energy Analysis is a non-deterministic methodology and an alternative way of calculating the structure response at high frequencies, applied to structures of larger dimensions.

The deterministic methods have the advantage of providing a more accurate response, besides allowing analysis of larger structures and higher frequencies. Also, it is possible to analyse just the frequency band of interest using deterministic models.

The existing models for beam reinforced plates mostly deal with plate models coupled to beam models. However, the beam models presented in the literature do not take into

account the wedge and web resonances. This work consists of determining the in-plane response and the transversal displacement of beam reinforced plates, allowing the calculation of the mean space response $\langle \overline{v^2} \rangle$, in frequency bands, using a deterministic model. Beams are treated as coupled plates and the response is determined analytically. For the correction prediction of the structure's response, it is necessary to obtain the frequency response function, for example the mobility function, along the coupling joint line. It is then necessary, in a first approach, to develop a beam model considering the out-of-plane and in-plane waves for the web and wedge resonances.

Although some experiments corroborate the analytical models, which take into account just the out-of-plane waves, many studies in this area resulted in expressive differences between experimental results and those obtained from models based only on flexural waves. In this case, the shear coefficient, rotary inertia and the presence of in-plane waves are indicated as the cause of this divergence.

The theory most commonly used to describe the plate problem is the thin plate theory. This theory produces good results when the wavelength is much larger than the thickness of the plate. The thin plate theory is applied to flexural plane waves propagating in an elastic solid which has a dimension much smaller than the other two dimensions. The wave theory that complements the in-plane waves is extensional wave analysis of thin plates, which describes the motion of the “quasi longitudinal” shear waves. The main hypothesis, in both formulations, is that the normal stress, σ_{zz} , is zero, and the line normal to the plane remains normal and straight after deformation.

When the wavelength is of the same order as the plate thickness, other more precise theories can be applied, such as the theories of Reissner [4], Uflyand [5] and Mindlin [6]. The latter represents an evolution of the thin plate theory approximation, since it includes the shear

stress effect in the plate. The applicability is limited to frequencies up to the first shear mode of the plate. This limitation is a consequence of the fact that the equations are based on the hypothesis that a line straight and normal to the neutral line remains straight, but not necessarily normal, after deformation, i.e., it is assumed that shear stress is linearly distributed across the plate thickness. In Mindlin's [6] formulation for bending waves, two slope functions, one in each coordinate direction of the plate plane, are defined analogous to the slope functions used in the one dimensional beam theory developed by Timoshenko [7], where a correction factor is used.

Leissa [8], in 1969, carried out a very valuable study on plate vibration. It consists of the analytical results of several rectangular plate geometries submitted to different boundary conditions. Most of the results are natural frequencies of plates. Parametric results of natural frequencies are also presented depending on the dimension of the plate, material density and Young's Modulus.

Cremer and Heckl [9], in 1973, presented in their classic book on structural acoustics important basic concepts on vibrations and sound radiation from beams and plates. Basic concepts related to longitudinal, in-plane, torsional and flexural waves are presented. The theory behind obtaining transmission coefficients for normal and random incidence may be found there. These coefficients are applied in Statistical Energy Analysis to determine the coupling loss factors between sound fields and plate-like structural components.

Hwang and Pi [2], in 1973, investigated the mechanism of power flow between connected plates, using the Mindlin theory to model the plate vibration problem. In space vehicles structures, it is usually assumed that the power flow at high frequencies is due to bending and shear waves, and the tension and compression effects are considered to contribute minimally to the energy transfer. The major parameters affecting the magnitudes and modes of energy transfer include the geometry of the substructures, their boundary

conditions, interface configurations (length, geometry, method of fabrication, etc), coupling loss factors, modal densities of the connected structures, and location and type of loading. These authors made a number of simple test models featuring certain basic similarities in order to sort out the various parameters and to reach a rational solution to this complex problem.

In a given connected structure [2], the degree of modal diffusion depends greatly on the wavelength in relation to the characteristic dimensions of the structure and on its thickness. As the stress waves propagate over the structure, the boundaries and interfaces cause a partial or total reflection of the waves. The infinitely numerous possibilities for wave propagation and reflection cause a randomly distributed wave pattern (high degree of modal diffusion). For waves of medium or long length, the degree of diffusion affects the energy transfer through an interface because the directional properties of the waves determine the amount of energy transmitted to the neighbouring structure. The effect is believed to be less pronounced for shorter-length waves.

In 1983, the effect of in-plane waves was analyzed by Lyon [10]. It is usually assumed that the flexural modes are dominant in energy transmission since they have a better coupling with the sound field. This is correct only for directly excited structures or structures with few coupled structural components. However, Lyon showed that when transmission occurs through various components, the energy transmission by longitudinal and shear waves must be considered, otherwise considerable errors in the structural energy transmission analysis will be introduced.

Hagedorn [11], in 1968, reported a study on the response of aerospace structures. This type of structure has appendices such as flanges and ribs, in some cases modelled as beams and in others as thin plates or shells. In his work, the impedance matrix necessary to

accurately describe the dynamic behaviour of rectangular plates with free edge boundary conditions was derived.

Cuschieri and McCollum [12], in 1990, analysed the power flow through the joint line between thick connected plates, considering out of plane and in-plane waves. The results were used in a SEA model analysis. The rotary inertia of plates and the shear effect according to Mindlin [6] theory were considered. It was concluded that in terms of power flow through the junction of an L shaped plate, where the two sides of the plate are identical, the rotary inertia along with the effects of shear and in-plane waves have a great influence. Considering only the out of plane waves, an overestimated power flow was observed at high frequencies and for thick plates. For a pinned junction, where there is no in-plane wave motion, an analysis based on pure bending indicated a significant overestimation of the power transmission through the junction, especially at high frequencies and for thick plates ($k h > 0.3$). For an unconstrained junction and for identical thickness plates, the thick plate bending effects are still important. However, for values of $k h > 1.0$, the in-plane waves produce an additional coupling mechanism between the plates, increasing the significance of this in-plane coupling and wave transmission as frequency increases. For plates of different thicknesses, the influence of shear and rotary inertia on the power transmission becomes less pronounced, while the influence of in-plane wave generation is similar to the identical plates case.

Cuschieri and McCollum [13] used the Mobility Power Flow approach to determine the structural power flow through the junctions between two flat plates, coupled in an L-shaped configuration, for both in-plane and out-of-plane (bending) waves propagation. Power flow by both types of waves is included by considering the junction edge between the two plates to be free. The results of the analysis show that the in-plane waves do not significantly contribute to the structural power flow at relatively low frequencies, that is, for frequencies below a bending wave number and plate thickness product of approximately 0.1. One of the

relevant results, in this case, is that the power flow results are not different from those obtained if the junction is assumed to be pinned, and power is transmitted only by out-of-plane waves. However, as the frequency increases, and for a bending wave number and plate thickness products greater than approximately 1.0, the contribution from the in-plane waves dominates.

Another important conclusion from their work is with regard to the frequency range where in-plane waves dominate. In-plane longitudinal are more significant than in-plane shear waves, although this has some dependence on the selected L-shaped configuration. The results of the analysis show that for low frequencies, kh less than approximately 0.16, the in-plane waves do not play a significant role in the transfer of power across the junctions of the L-shaped plate structure. The in-plane waves can be neglected without any loss of accuracy in the power flow results. The importance of the in-plane waves as a mechanism for the transfer of vibrational power across the junction, increases as the frequency increases. For kh greater than approximately 1.0, the power transferred by the in-plane waves dominates over that transferred by the out-of-plane waves. Comparing vibrational power transferred by the two in-plane wave components, the in-plane longitudinal waves seem to transfer more power than the in-plane shear waves. The inclusion of in-plane waves reduces the predicted value for the transferred power ratio. This is due to the fact that the in-plane waves transport some of the power back to the source plate, while pure bending modelling overestimates the predicted value of the power ratio.

Cuschieri [14] performed also a power flow parametric analysis through thin plates coupled in L shape, varying parameters, such as thickness, area, material properties, structural loss factor and external load distribution. A comparison between power flow method and Statistical Energy Analysis (SEA) results showed good agreement.

Bercin [15], in 1996, analysed the contribution of the in-plane waves to the power flow, using the dynamic stiffness method, which leads to exact responses for certain types of structures. The fundamental difference between this technique and the Finite Element Method is that in the latter the movement differential equation is solved exactly for each frequency ω . In this work, it is shown that the exclusion of the in-plane waves can lead to large errors in the energy prediction, unless applied to very simple structures.

Baars [16] used the Mobility Method to determine the Power Flow between two coupled beams. It was analysed the structural damping and stiffness effects on the power flow and between structural components, input power and vibratory energy response. A methodology for experimental determination of the input power and power flow is also presented.

The works reported by Clarkson [17], [18], [19], describe and present results of an experimental technique for the determination of coupling loss factors, modal density and structural loss factors of coupled structural components. The proposed *in situ* technique has a great advantage of being able to determine the actual loss factors of coupled components, which includes the dissipation at the joint line, and the coupling loss factors produced by complex joints, such as made by rivets or bolts.

Ozelame [20] , in 1997, used Finite Element to analyse the modal densities and coupling loss factors for plates reinforced by beams considering out-of-plane (bending) waves only. The main conclusion is that the coupling loss factors are fairly constants with frequency. The reinforcing beams were modelled as Euler and Timoshenko beams.

Bonilha [21], in 1996, developed a hybrid deterministic-probabilistic model for Vibroacoustic studies to analyse the acoustic field inside a hard-walled acoustic cavity due to the random vibration of one flexible wall. In his work it was verified that the hybrid model results approached closely those from a SEA model as the modal density of both systems is

increased. The proposed model results agreed well with Finite Element results in the lower frequency range, where both systems are modally-sparse. Narrow band and frequency averaged sound pressure level obtained approach closely the experimental results as long as more than eight plate modes are available in a frequency band or the plate model overlap factor is higher than unity.

Litwinczik [22], in 1997, analysed the effects of a reinforcing beam on sound radiation from plates vibrating in bending modes. It was concluded that the radiation efficiency is largely dependent upon the space symmetry of the vibrating modes, due to cancellation effects. This is more pronounced at low frequencies, where the sound wavelength is larger.

Bonifácio [23], in 2003, used a random analysis to predict the response of beams and plates subjected to different boundary conditions and to random excitation. The response was determined in frequency bands instead of discrete frequencies. Good results were obtained regarding processing time when compared to Finite Element Method.

Nunes [24], in 2002, developed a deterministic model to calculate the response of rectangular plates reinforced by beams on the edge, subjected to free edge boundary conditions. It was evaluated the power flow through the structure using mobility functions. One of the conclusions of this work is that adding a beam at the plates joint line decreases the modal density of the system, due to a stiffening effect.

In 2003, Gouveia [25] used the Finite Element Model to analyse the influence of the skid of machines on Power Flow to the structure of offshore platforms. It was concluded that the reinforcing beams have a great influence on the energy absorbed by the plate. The greater the beam stiffness, the lower the power flow transmitted to the plate.

Fiates [26], in 2003, used a Finite Element Method to calculate a beam reinforced plate velocity and calculated the sound pressure field generated by this velocities. In this work, the beam was modeled as plate elements, considering their own modes of web and

wedge. Using an optimization routine, the ideal shape of the beam was determined as a recommendation to minimize the plate sound radiation.

Yoneda [27], in 2002, developed a methodology for determining the transmission loss for plate reinforced beams through the Finite Element Method. In his work, it was concluded that the reinforcing beams decrease the transmission loss at low frequencies.

Heron [28], in 1997, developed a calculation procedure for a general line connection of plates. It is based on the use of line wave impedance matrices, analogous to the use of point impedance matrices for beam networks. The problem associated with plates attached along different lines of the beam section, such as the opposite flanges of an I-beam, is best solved by modelling the beam as a series of strip plate elements rather than introducing a special six degrees of freedom element as cited in Langley and Heron [29]. In the vast majority of applications beams are thin sectioned and should be modelled as a series of strip plates in order to accurately predict the beam dynamics at mid and high frequencies. In Heron's work, he concluded that treating the full I-beam as a beam is a good model at lower frequencies but introduces errors that exceed 10 dB at frequencies above 1 kHz. It was also concluded that the strip plate model is remarkably accurate over the whole frequency range.

In 1996, Fiates [30] applied the Mobility Functions approach to structures composed of beams arranged in a grill configuration. In his work, he analysed the contribution of longitudinal, bending and torsional waves to the power flow. It was concluded that longitudinal waves are important when considering beams of greater length and at high frequencies. The torsional waves are responsible for the transmission of a considerable portion of energy when compared with flexural (bending) waves. On the other hand, for beams with shorter lengths, the shear effect on flexural waves must be considered. The methodology used by this author is analytical, allowing the deterministic response for the whole the frequency spectrum.

Bonifácio [31], in 1998, also used the Mobility approach to analyse the flexural wave response of coupled plates, and determined the flow of vibratory energy transmitted through the plate joints, assessing the effects of the main related parameters. In his work, the power flow of two plates were analysed and the analysis was then extended to plates having a beam in the joint. Plate bending waves were modelled by thin plate theory. He verified that the parameters related to the beam modify significantly the magnitude and frequency of the power flow between plates.

Farag and Pan [32], in 1998, developed a model for the coupling of two finite plates connected at an arbitrary angle for the prediction of the dynamic response and power flow at the coupling edge and at any cross section. The coupling at the joint edge considers bending, out-of-plane shear and in-plane longitudinal vibration and no constraint is imposed on the in-plane displacement perpendicular to the coupling edge. The exact solution for free flexural mode shapes and resonance frequencies of rectangular plates with one free edge and the other edges simply supported is considered in their work. This exact solution satisfies both the displacement and force boundary conditions, and, consequently, it is used in the coupling of flat panels. Farag and Pan presented an approximate solution for the in-plane response of the same plate panels when excited by in-plane forces perpendicular to the free edge. They also showed that the coupling of two plates is mainly due to the moment at frequencies up to the cut-off frequency of the first in-plane mode. Above this frequency, the coupling is due to out-of-plane shear and in-plane vibration with a diminishing participation of the moment in transmitting vibrational power through the coupling edge.

Farag and Pan [33] also developed a mathematical model to predict forced response for in-plane point force excitations. They showed the nature of the coupling between in-plane longitudinal and in-plane shear waves and the resonance characteristics of the in-plane vibrational behaviour of finite flat plates. They concluded that the input power due to in-plane

force excitation at the in-plane resonance frequencies is at the same level as that due to out-of-plane force excitations for the flexural resonances in the same frequency band.

Langley and Bremmer [34], in 1999, presented a new method for dynamic systems analysis based on the partitioning of the system's degrees of freedom into a global and a local set. The global equation of movement is formulated and solved in a traditional way while the local degrees of freedom are formulated and treated using Statistical Energy Analysis, using the input power of the global degrees of freedom. This method gives good results in the low and high frequency regions.

Souza [35], in 2000, applied, computationally, the Mobility Method to structures like beams arranged in a grill shape. They concluded that bending waves concentrate a large amount of vibratory energy. However, longitudinal and torsional waves are important in the power transmission.

Gunda et al [36] applied the Image Method or ray tracing techniques in order to analyse the harmonic response of beams and rectangular plates. The fundamental solution for an infinite plate was employed, in conjunction with appropriately placed images, to obtain the dynamic response of simply supported rectangular plates over a wide range of frequencies. In their work, simply supported beams were analysed firstly by considering the fundamental solution of an infinite beam, and secondly for the case of a narrow plate with simply supported and roller boundary conditions. They concluded that both approaches closely match the closed form solutions and with measurements taken for two beams.

The distribution of vibration over finite structures excited by a force was considered by Petersson [37]. To describe the vibration distribution a parameter called motion transmissibility was introduced, defined as the ratio of the velocity of the structure at an arbitrary point to that at the excitation location. It was found that for rods, beams and shells, the motion transmissibility can be estimated by using the corresponding semi-infinite

structure. For plates, the motion transmissibility can be estimated by considering the corresponding quarter-infinite structure. This method can also be applied to inhomogeneous boundary conditions, using a correction term which accounts for free boundary conditions [38].

In 1999, Sardá [39] analysed the power flow mechanism between two flat plates supported by beams using the Finite Element Method. The contribution of the beams and the plates to the transmission and the several paths was analysed. The contribution of each type of strength (internal forces or moments), associated with the corresponding velocities, to the power flow was studied. The coupling loss factor behaviour for plates supported by beams, according to the cross sections and dimensions used for the beams, was also analysed. Significant differences in the coupling loss factor, vibratory energy and power flow, when beams are modelled as beam elements or as plate elements, were observed, since elements take into account beam web and wedge resonances, resulting in a more accurate model. The analyses were made using ANSYS, version 5.3, up to 1000 Hz. In his work, plates with dimensions of 2 m² were used, where the first plate had 1.1 m length and the second 0.9 m length, both with a thickness of 5 mm. The Finite Element mesh size was 2.9 cm, and the analysis had, approximately, 2500 elements and 2600 nodes. The processing time for calculating all the parameters, such as power flow, vibratory energy and input power, oscillated between 12 hours and 20 hours, when using a computer Pentium Pro 200 MHz, with a 2.1 Gb hard disk and 64 Mb RAM.

Sardá analysed different configurations of plates supported by stiff beams and flexible beams, arranged in a horizontal plane, where the terms stiff and flexible relate to beams modelled by the beam element or plate element, respectively.

The plates were modelled with SHELL 63 [40] from the ANSYS library. This element has four nodes and six degrees of freedom per node, three for translation and three for

rotation. The beams used as plate supports were modelled with the beam element BEAM 44 [41] and the plate element SHELL 63, and results from both cases were compared. Figure 1.2 shows the geometry analysed, and the boundary condition used. The excitation consists of several point forces distributed over the first plate. In this specific case, several unit forces with random phase differences were used. Figures 1.3 and 1.4 show the Finite Element mesh used, considering beams modelled as plate elements.

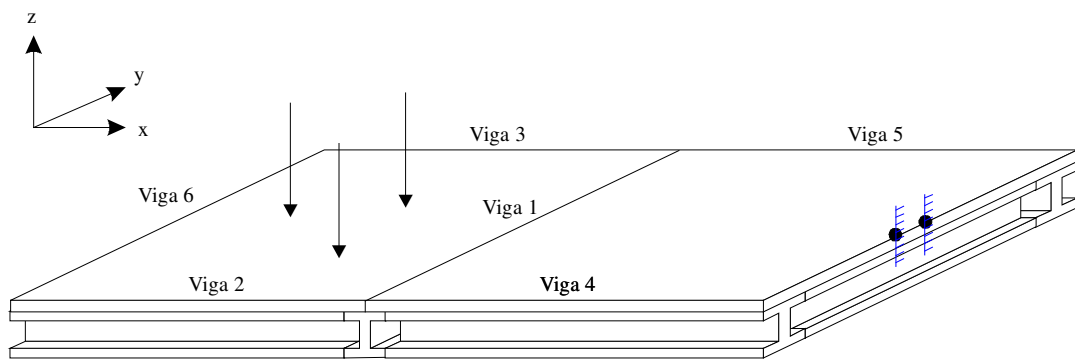


Figure 1.2 – Boundary condition used – two clamped nodes

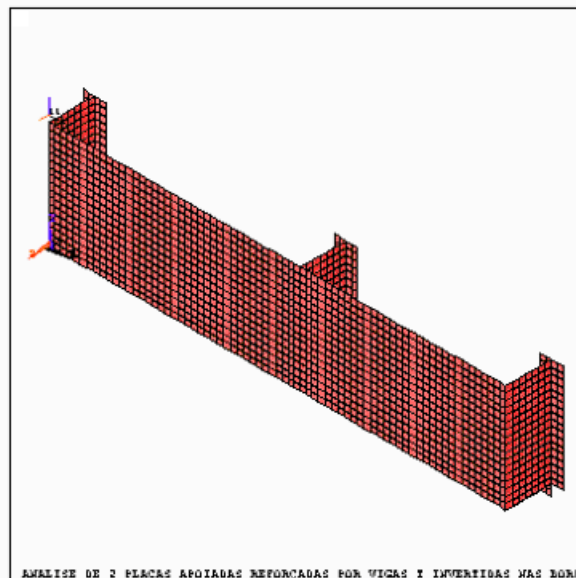


Figure 1.3 – View of the beam reinforced model plate Finite Element Mesh.

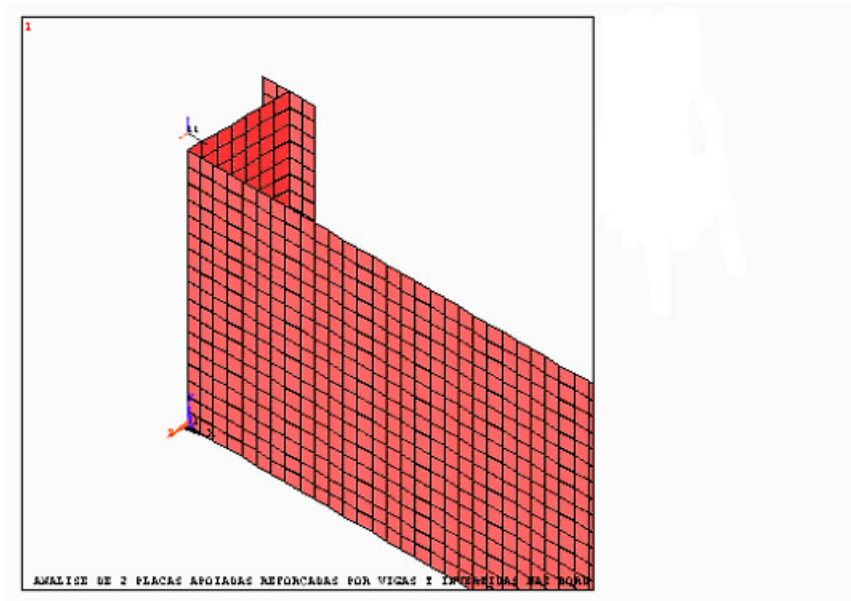


Figure 1.4 – Detailed view of the beam reinforced plate model Finite Element Mesh.

For the geometries analysed, it was noticed that the greater the height of the beam in relation to the beam length, the greater the difference between the coupling loss factors obtained for beams modelled as beam or plate elements. It was observed, for example, that for plates with beams at the junction, the power flow spectrum is totally different at high frequencies for the two considered models. For the case where the beam was modelled as a plate element, it was noticed that more energy is transmitted, which can be explained by the fact that this model has less stiffness at the junction of the plates. Other differences could be associated with wedge and web resonances. This is shown in Figures 1.5 and 1.6. It can be observed that for an inverted T beam with 5 cm height this difference in power is not so evident. However, for the 20 cm height beam, the difference in the power flow is very significant. The same is true for coupling loss factors, as seen in Figures 1.7 and 1.8.

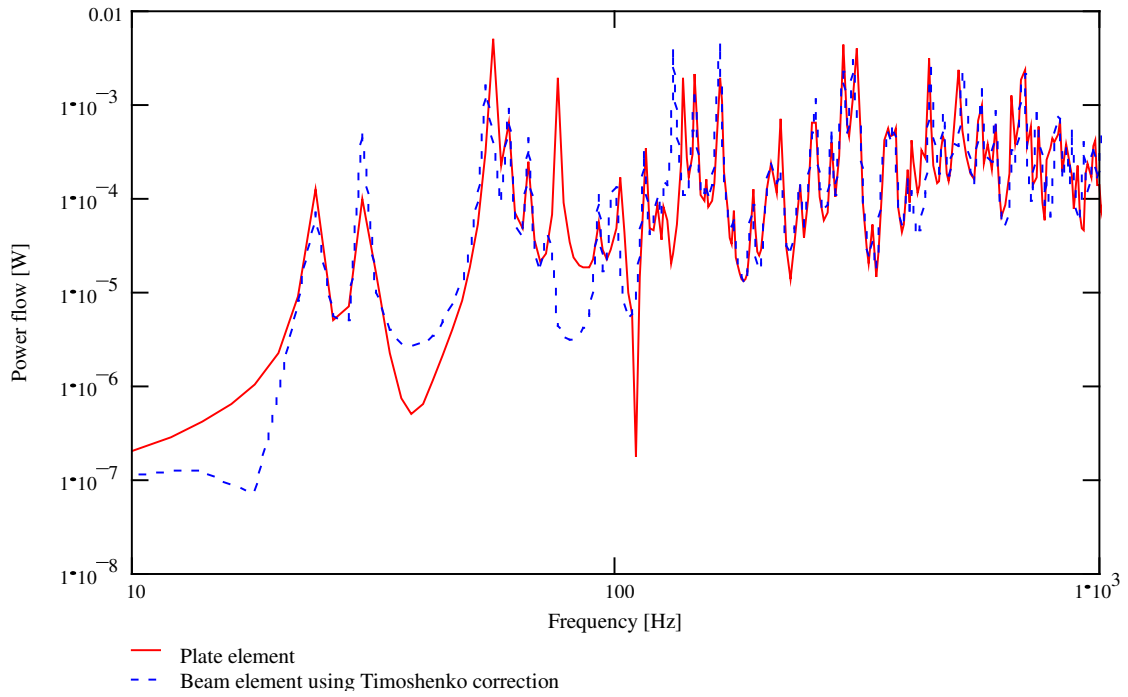


Figure 1.5 – Power flow between subsystems 1 and 2. Comparison between plate element and beam element, inverted T beam, 5 cm height; base 2.5 cm; thickness 0.25 cm.

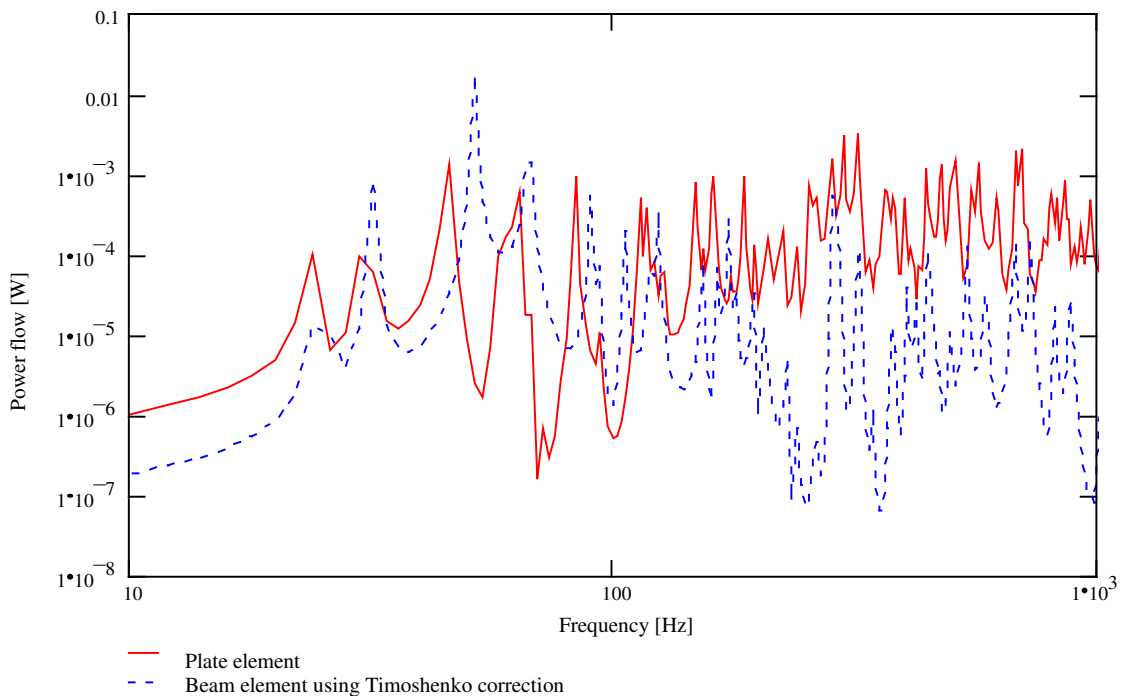


Figure 1.6 – Power flow between subsystems 1 and 2. Comparison between plate element and beam element, inverted T beam, 20 cm height; base 10.0 cm; thickness 1.0 cm.

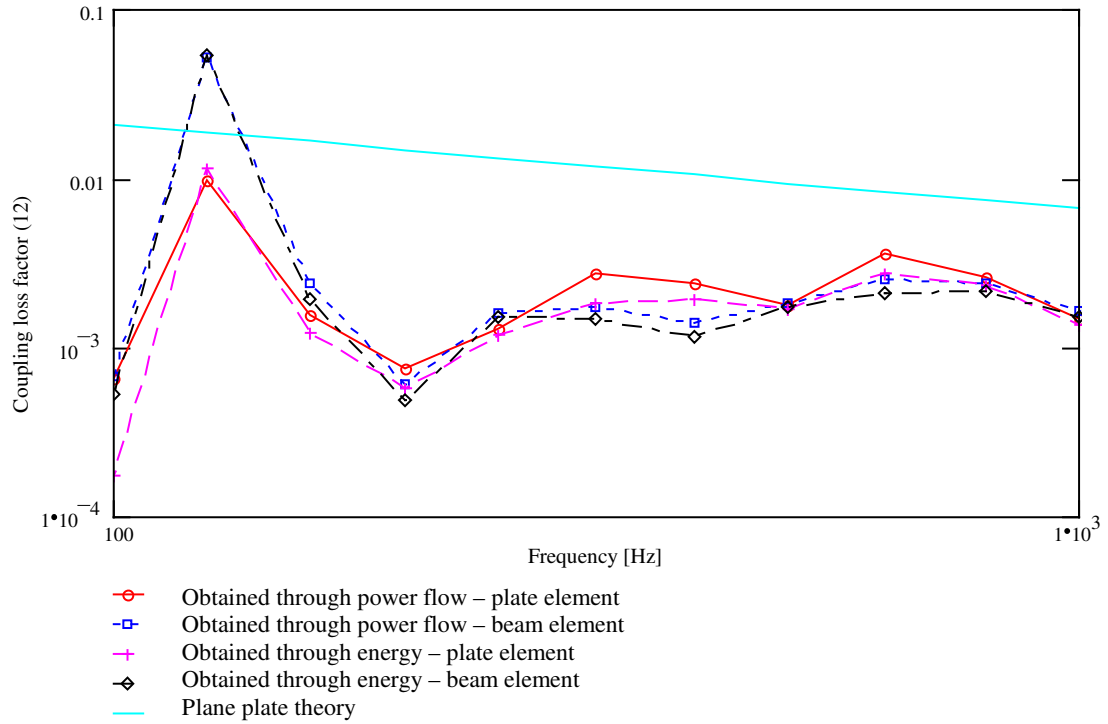


Figure 1.7 – Coupling loss factor for subsystems 1 and 2. Comparison between plate element and beam element, inverted T beam, 5 cm height; base 2.5 cm; thickness 0.25 cm.

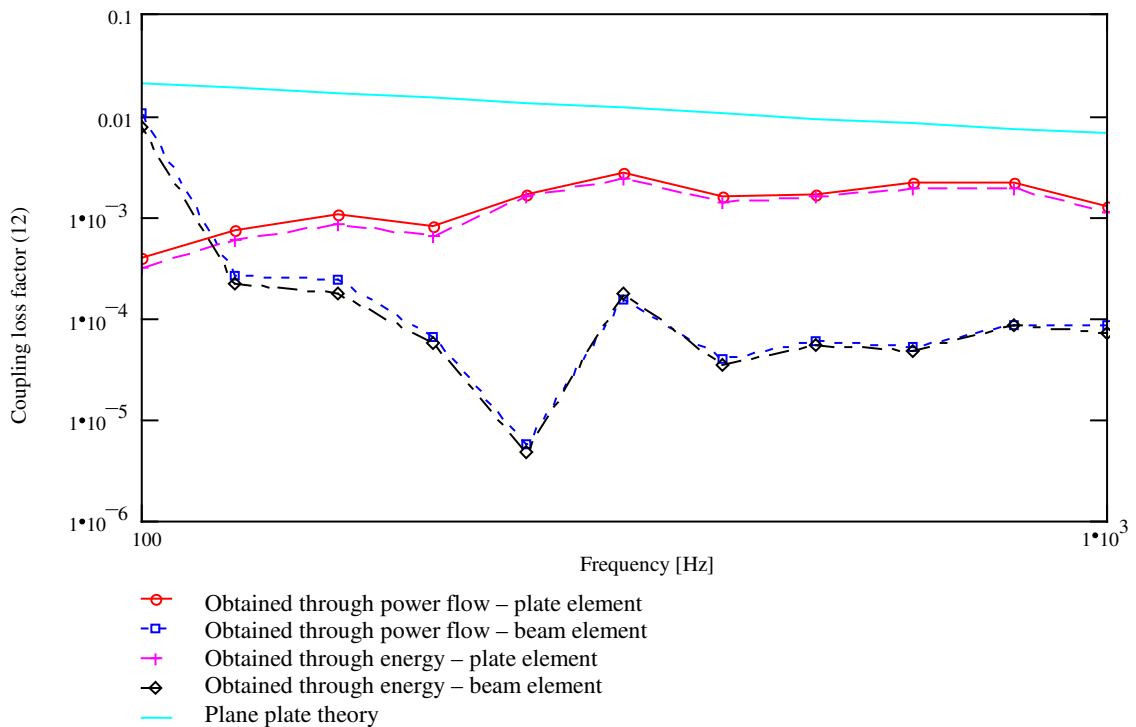


Figure 1.8 – Coupling loss factor for subsystems 1 and 2. Comparison between plate element and beam element, inverted T beam, 20 cm height; base 10.0 cm; thickness 1.0 cm.

It should be noted that the above mentioned studies take into account models in which the web and wedge modes were not considered. From the work by Sardá, it can be concluded that for a more accurate prediction of the power flow and the coupling loss factors for beam reinforced plates, a plate model for the beams must be used, considering the web and wedge modes. It was observed, too, that the Finite Element Method, for this type of structure, has a limitation regarding the processing time at high frequencies. These results set the ground work for the present study. Its objective is to develop a model for large structures that has an acceptable processing time and takes into account the web and wedge resonances.

The main objective of this work consists of developing a deterministic model for vibrations of inverted T and L beams, taking into account the out-of-plane and in-plane waves, and using this model as a support of two connected plates. This model will be validated through comparison to the Finite Element Method.

Other methods for determining the mobility of plates will also be presented. One method is the Image Method, which involves the correct placing of sources and images of vibrations on a plate to obtain the final response.

Chapter 2 describes some basic concepts regarding the vibration of plates. It describes how to obtain the differential equations for in-plane and out-of-plane vibration and the boundary condition used.

In Chapter 3 the solutions for the in-plane and out-of-plane wave problems are found. The in-plane solution is described as two propagating waves, one solution propagating in the positive x direction and the other in the negative direction. For out-of-plane waves, the differential equation is solved in terms of base functions, since in the y direction and propagating waves in the x direction. In this chapter, the analytical out-of-plane and in-plane solutions are used to determine the response of an L plate and a T plate configuration problem.

In Chapter 4 the Image Method is described. This method is an alternative for determining Mobility functions for plates. The advantage of the method is its accuracy and the fast obtaintion of results when applied to larger plates and high structural damping. In this chapter a solution, based on a series, is used to solve the response of a three dimensional parallelepiped and the results are compared with the solution obtained analytically.

In Chapter 5 an analytical model of two connected plates with an L beam, modelled using plate equations, is developed. This model considers the in-plane and the out-of-plane waves. The results obtained are considered good when compared with a Finite Element Model, and the advantage is that it can be used for large plates and at high frequencies. Application of the model is very fast when compared with a Finite Element Method.

Chapter 6 presents the conclusions for the current work and suggestions for future works.

CHAPTER 6

CONCLUSIONS

Procedures for the determination of the response of beam reinforced plates including in-plane and out-of-plane waves were presented in this work. The proposed models include the analytical solution, the Image Method and a model for vibration of a three dimensional parallelepiped, where the latter method can be used for determination of mobilities for free-free edge boundary conditions for plates and beams.

Chapter two presented basic concepts on plate vibration, showing the derivation of the differential equations of in-plane and the out-of-plane waves motion. The different boundary conditions for thin plates were also presented.

Chapter three presented the in-plane and the out-of-plane waves solution for a bi-supported rectangular plate in an analytical form, consisting of propagating and evanescent waves. Both solutions were coupled to correctly represent solutions for transversal and in-plane displacements for L and T beams with a distributed applied load. The solutions of the models were fast and results were accurate. These observations represent the main advantages

of using this method. The presented models can be used in impedance input values determination for future analyses for vibrations prediction of reinforced plates.

As an alternative to the analytical formulation, the Method of Images and the assumed solution for a three dimensional parallelepiped were found to be efficient. It was shown that the Image Method works very well for large plates and the accuracy of the method increases when the plate becomes larger. The number of images to be used for large plates tends to decrease, making the method faster for larger structures. It works better for high frequencies, where the accuracy is better for the same number of images. This method is applicable to different plate boundary conditions, provided the correction factor is calculated. An alternative solution for determining the mobilities of a free-free plate or free-free beam using the solution obtained for a three dimensional parallelepiped was shown.

A very valuable model for two connected bi-supported plates with a beam on the joint line was presented in Chapter five. A model representing the in-plane and out-of-plane waves for all connected plates is shown. This model takes into account the web and wedge resonances of the beam (modeled as connected plates). This method was shown to be very fast and can be used to obtain coupling loss factors of beam reinforced plates.

As shown in Chapter 5, the importance of considering the in-plane effects and the beam own modes was presented, otherwise the calculated response and power flow could not take into account the effect of the resonances of the beam web and wedge. This procedure can generate more accurate results for power flow analysis, and consequently, to coupling loss factors calculations.

The analytical method can be used for determining the response of reinforced plates with larger dimensions compared with the Finite Element Method. The advantage of this method is related to the fast calculations with which the response is obtained, for in-plane and out-of-plane waves. The model for two connected plates with an L beam on the joint line can

be easily used to obtain the coupling loss factors for reinforced structures and also in Statistical Energy Analysis calculations.

SUGGESTIONS FOR FUTURE WORKS

For future works the determination of coupling loss factors of beam reinforced plates using the Analytical Method is suggested, as well as the use of the results in Statistical Energy Analysis models to predict vibrations of this type of structures. The analysis of larger structures having a number of reinforcing beams is also recommended.

An analysis of the power flow between beam reinforced plates is suggested. In this case, the model could be used to calculate the internal loads on the structure and the respective velocities. With this data, the power flow can be easily calculated and analyzed.

The use of the Image Method and the solution for the three-dimensional parallelepiped to obtain the Mobilities can be employed as an alternative to the analytical solution. The solution developed for a transversal force and a moment applied to a plate can be used as an alternative for determining the mobility functions to be used in the plate connection. The calculation of the coupling loss factor for large structures could be carried out using these methods.

REFERENCES

- [1] LYON, R. H., “Statistical energy analysis of dynamical systems”, MIT Press, Massachusetts, 1975.
- [2] HWANG, C. and PI, W.S., “Investigation of Vibrational Energy Transfer in Connected Structures”, NASA-CR-124450, Final Report, 1972.
- [3] LENZI, A., “Análise Estatística Energética – SEA”, Mechanical Engineer Graduate Course Notes, Federal University of Santa Catarina, 1996.
- [4] REISSNER, E. “The effect of transverse shear deformation on the bending of elastic plates”, Journal of Applied Mechanics, vol. 12, pp. 69–77, 1945.
- [5] UFLYAND, Y. S. “The propagation of waves in the transverse vibration of bars and plates”, Prikl. Mat. Meh., vol. 12, pp. 287–300, 1948.
- [6] MINDLIN, R. D. “Influence of rotary inertia and shear on flexural motions of isotropic, elastic plates”, Journal of Applied Mechanics, vol. 18(3), pp. 31–38, March, 1951.
- [7] TIMOSHENKO, S. P., “Strength of materials”, Part 1, second edition, D. Van Nostrand Company, Inc., New York, N. Y., 1940, pp. 170-171.
- [8] LEISSA, A. W., “Vibration of Plates”, Ohio State University, Columbus, Ohio, 1969.

- [9] CREMER, L., HECKL, M. and UNGAR, E. E., Structure-Borne Sound, Springer Verlag, Berlin, 1973.
- [10] LYON, R. H. "In-plane Contribution to Structural Noise Transmission", Transactions of the ASME, 60, pp. 123-130, March, 1983.
- [11] HAGEDORN, P., KELKEL, K., WALLASCHEK, J. "Vibrations and impedances of rectangular plates with free boundaries", Springer-Verlag, Berlin, 1986.
- [12] CUSCHIERI, J. M., "Bending and in-plane wave transmission in thick connected plates using statistical energy analysis", Journal of the Acoustical Society of America, vol.88 (3), pp. 1480 - 1485, 1990.
- [13] CUSCHIERI, J. M., "In-Plane and out-of-plane waves power transmission through an L-plate junction using the mobility power flow approach", Journal of the Acoustical Society of America, vol.100 (1), pp. 857 - 870, 1996.
- [14] CUSCHIERI, J. M., "Parametric analysis of the power flow on an L-shaped plate using a mobility power flow approach", Journal of the Acoustical Society of American- vol.91 (5), pp. 2686 - 2695, 1992.
- [15] BERCIN, A. N. "An assessment of the effects of in-plane vibrations on the energy flow between coupled plates", Journal of Sound and Vibration, 191(5), pp. 661-680, 1996.
- [16] BAARS, E., "Fluxo de potência vibratória em componentes estruturais tipo barras e vigas", M.Sc. Thesis, Federal University of Santa Catarina, 1996.
- [17] CLARKSON, B. L., POPE, R.J., "Experimental determination of modal densities and loss factors of flat plates and cylinders", Journal of Sound and Vibration, 77(4), pp. 535-549, 1981.

- [18] CLARKSON, B. L., POPE, R.J., “Estimation of the coupling loss factor of structural joints”, *Journal of Mechanical Engineering Science*, 205, pp. 17-22, 1991.
- [19] CLARKSON, B. L., RANKY, M. F., “On the measurement of the coupling loss factors of structural connections”, *Journal of Sound and Vibration*, vol. 94, pp. 249-261, 1984.
- [20] OZELAME, A. E., “Análise de densidade modal e de fatores de acoplamento para placas reforçadas por vigas”, M.Sc. Thesis, Federal University of Santa Catarina, 1997.
- [21] BONILHA, M. W., “A hybrid deterministic-probabilistic model for vibroacoustics studies”, Ph.D. Thesis, Institute of Sound and Vibration Research, 1996.
- [22] LITWINCZIK, V., “Irradiação sonora de placas planas com descontinuidade”, M.Sc. Thesis, Federal University of Santa Catarina, Brasil, 1998.
- [23] BONIFÁCIO, P. R., “Vibração aleatória de placas finas retangulares, vigas e estruturas acopladas”, Ph.D. Thesis, Federal University of Santa Catarina, Brasil, 2003
- [24] NUNES, M. A. C., “Vibrações de placas e vigas acopladas pelo método da mobilidade”, Ph.D. Thesis, Federal University of Santa Catarina, Brasil , 2002.
- [25] GOUVEIA, V. L., “Fluxo de energia vibratória através da base de fixação de máquinas para a estrutura de plataformas offshore”, M.Sc. Thesis, Federal University of Santa Catarina, Brasil, 2003.
- [26] FIATES, F., “Radiação sonora de placas reforçadas por vigas”, Ph.D. Thesis, Federal University of Santa Catarina, Brasil, 2003
- [27] YONEDA, R., “Metodologia de cálculo de perda de transmissão de placas reforçadas por vigas”, M.Sc. Thesis, Federal University of Santa Catarina, Brasil, 2002.

- [28] HERON, K. H. “Predictive SEA using line wave impedance”, Symposium on Statistical Energy Analysis, Southampton, UK, July, 1997.
- [29] LANGLEY, R.S., HERON, K.H., “Elastic wave transmission through plate/beam junctions”, *Journal of Sound and Vibration*, 143(2), 241-253.
- [30] FIATES, F., “Análise de vibrações de componentes estruturais tipo vigas acopladas pelo método da mobilidade”, M.Sc. Thesis, Federal University of Santa Catarina, Brasil, 1996.
- [31] BONIFÁCIO, P. R., “Análise do Fluxo de Energia Vibratória entre Placas Retangulares Simplesmente Apoiadas pelo Método da Mobilidade”, M.Sc. Thesis, Federal University of Santa Catarina, Brasil, 1998.
- [32] FARAG, N. H., PAN, J. “On the free and forced vibration of single and coupled rectangular plates”, *Journal of the Acoustical Society of America*, vol. 104(1), pp. 204-216, 1998.
- [33] FARAG, N. H., PAN, J. “Free and forced in-plane vibration of rectangular plates”, *Journal of the Acoustical Society of America*, vol. 103(1), pp. 408-413, 1998.
- [34] LANGLEY, R. S., P. BREMNER, “A hybrid method for the vibration analysis of complex structural-acoustic systems”, *Journal of the Acoustical Society of America*, vol. 105(3), pp. 1657–1671, 1999.
- [35] SOUZA, L. C., “Respostas e fluxo de energia vibratória em estruturas compostas por vigas pelo método da mobilidade”, M.Sc. Thesis, Federal University of Santa Catarina, Brasil, 2000.
- [36] GUNDA, R., VIJAYAKAR, S. M., SINGH, R. “Method of images for the harmonic response of beams and rectangular plates”, *Journal of Sound and Vibration*, vol. 185(5), pp. 891 – 808, 1995.

- [37] LIANG, J., PETERSSON, B. A. T. “Estimation of vibration distribution for finite structures”, *Journal of Sound and Vibration*, vol. 238(2), pp. 271 – 293, 2000.
- [38] GUNDA, R., VIJAYAKAR, S. M., SINGH, R., FARSTAD, J. E., “Harmonic Green’s function of a semi-infinite plate with clamped or free edges”, *Journal of the Acoustical Society of America*, vol. 103, pp. 888 – 899.
- [39] SARDÁ, A. A. P., “Análise por Elementos Finitos do Fluxo de Energia Vibratória Entre Placas Planas Apoiadas em Vigas”, M.Sc. Thesis, Federal University of Santa Catarina, Brasil, 1999.
- [40] ANSYS User’s Manual for Revision 5.3– Elements, Swanson Analysis, Inc. 1995, pp. 465-472.
- [41] ANSYS User’s Manual for Revision 5.3– Theory, Swanson Analysis, Inc. 1995, pp. 11-19.
- [42] GRAFF, K. F., “Wave motion in elastic solids”, Dover Publications, New York, 1991.
- [43] FLÜGGE, W., “Stresses in Shells”, Springer-Verlag, Berlin, 1966.
- [45] MCCOLLUM, M. D., “Vibration power flow in thick connected plates”, Ph.D. Thesis, Florida Atlantic University, 1988.
- [46] CHEN, G., COLEMAN, M.P., ZHOU, J., “Analysis of vibration eigen frequencies of a thin plate by the Keller-Rubinow wave method: clamped boundary conditions with rectangular or circular geometry”, *Journal on Applied Mathematics*, vol. 51, pp. 967 – 983.

- [47] NYWA, Y., KOBAYASHI, S., KITAHARA, M., “Eigen frequency analysis of plate by the integral equation method”, *Theoretical and Applied Mechanics*, vol. 29, pp. 287 – 367.
- [48] SOMMERFELD, A., *Partial Differential Equations in Physics*, Academic Press, New York, 1964.
- [49] GOYDER, H. G. D., WHITE, R.G., “Vibrational power flow machines into build-up structures, part I : Introduction and approximate analyses of beam and plate-like foundations ”, *Journal on Sound and Vibration*, vol. 68(1), pp. 59–75.
- [50] ZILLMER, S.C. “Vibrations of a free rectangular parallelepiped”, M.Sc. Thesis, University of California, 1980.
- [51] HUTCHINSON, J.R., ZILLMER, S.C. “Vibration of a free rectangular parallelepiped”, *Journal of Applied Mechanics*, vol. 50, pp. 123-130, 1983.
- [52] GENTLEMAN, W. M. “Clenshaw-Curtis quadrature”, *Collected algorithms from CACM*, University of Waterloo, 1971.
- [53] GENTLEMAN, W. M. “Implementing Clenshaw-Curtis quadrature”, I Methodology and experience. *Comm. ACM* 15 (May 1972), 337-342.
- [54] GENTLEMAN, W. M. “Implementing Clenshaw-Curtis quadrature”, II Computing the cosine transformation *Comm. ACM* 15 (May 1972), 343-346.

APPENDIX A

DERIVATION OF THE EXPRESSIONS FOR θ , Q_y , AND M

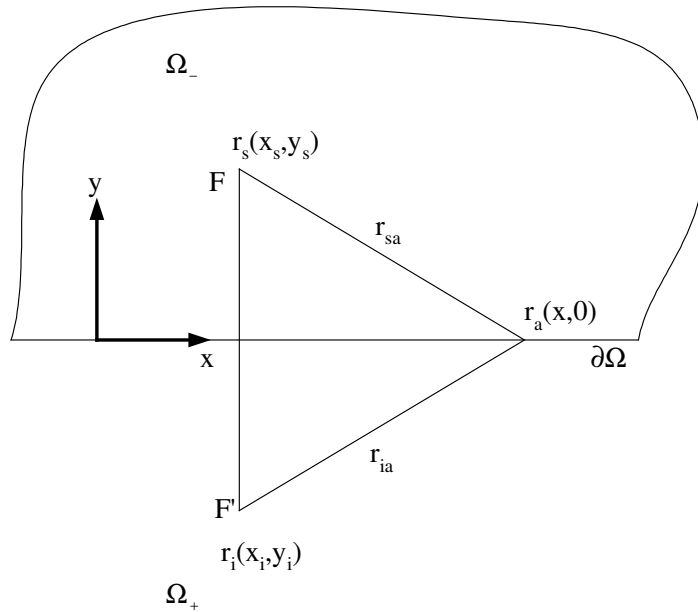


Figure A.1 – Imaging for semi-infinite plate.

The distance r can be written as:

$$r = \sqrt{(x - x_s)^2 + (y - y_s)^2} \quad (\text{A.1})$$

The derivatives of r can be written as:

$$\frac{\partial r}{\partial y} = \frac{1}{2} [(x - x_s)^2 + (y - y_s)^2]^{-\frac{1}{2}} 2(y - y_s) = \frac{y - y_s}{r} \quad (\text{A.2})$$

$$\frac{\partial^2 r}{\partial y^2} = \frac{\partial}{\partial y} \left[\frac{y - y_s}{r} \right] = \frac{\partial}{\partial y} \left\{ (y - y_s) [(x - x_s)^2 + (y - y_s)^2]^{-\frac{1}{2}} \right\} \quad (\text{A.3})$$

$$\frac{\partial^2 r}{\partial y^2} = 1 \left[(x - x_s)^2 + (y - y_s)^2 \right]^{\frac{1}{2}} + \quad (\text{A.4})$$

$$(y - y_s) \left(-\frac{1}{2} \right) \left[(x - x_s)^2 + (y - y_s)^2 \right]^{\frac{3}{2}} 2(y - y_s)$$

$$\frac{\partial^2 r}{\partial y^2} = \frac{1}{r} - \frac{(y - y_s)^2}{r^3} \quad (\text{A.5})$$

Similarly:

$$\frac{\partial r}{\partial x} = \frac{x - x_s}{r} \quad (\text{A.6})$$

$$\frac{\partial^2 r}{\partial x^2} = \frac{1}{r} - \frac{(x - x_s)^2}{r^3} \quad (\text{A.7})$$

The normal slope can be calculated as:

$$\theta_x = \frac{\partial u}{\partial y} = \frac{\partial u}{\partial r} \frac{\partial r}{\partial y} \quad (\text{A.8})$$

Then

$$\theta_x = \left(\frac{y - y_s}{r} \right) \left\{ \left(\frac{-j}{8\lambda^2 D} \right) \frac{\partial}{\partial r} \left[H_0^{(1)}(\lambda r) - H_0^{(1)}(j\lambda r) \right] \right\} \quad (\text{A.9})$$

Finally, for $y = 0$:

$$\theta_x = \frac{jy_s}{8\lambda^2 D r} \frac{\partial}{\partial r} \left[H_0^1(\lambda r) - H_0^1(j\lambda r) \right] \quad (\text{A.10})$$

The moment M_y can be determined using the expression given by Leissa [8]:

$$M_y = -D \left(\frac{\partial^2 w}{\partial y^2} + \nu \frac{\partial^2 w}{\partial x^2} \right) \quad (\text{A.11})$$

The derivatives can be calculated using:

$$\frac{\partial^2 w}{\partial y^2} = \frac{\partial}{\partial y} \left[\frac{\partial w}{\partial r} \frac{\partial r}{\partial y} \right] = \frac{\partial^2 w}{\partial y \partial r} \frac{\partial r}{\partial y} + \frac{\partial w}{\partial r} \frac{\partial^2 r}{\partial y^2} \quad (\text{A.12})$$

$$\frac{\partial^2 w}{\partial y \partial r} = \frac{\partial}{\partial r} \left(\frac{\partial w}{\partial y} \right) = \frac{\partial}{\partial r} \left(\frac{\partial w}{\partial r} \frac{\partial r}{\partial y} \right) \quad (\text{A.13})$$

$$\frac{\partial^2 w}{\partial y^2} = \frac{\partial}{\partial r} \left(\frac{\partial w}{\partial r} \frac{\partial r}{\partial y} \right) \frac{\partial r}{\partial y} + \frac{\partial w}{\partial r} \frac{\partial^2 r}{\partial y^2} \quad (\text{A.14})$$

Then, using the following expression:

$$\left(\frac{\partial w}{\partial r} \frac{\partial r}{\partial y}\right) = \frac{j}{8\lambda^2 D} \frac{\partial}{\partial r} [\Pi(\lambda r)] \left(\frac{y-y_s}{r}\right) \quad (\text{A.15})$$

Where

$$\Pi(\lambda r) = H_0^1(\lambda r) - H_0^1(j\lambda r) \quad (\text{A.16})$$

$$\frac{\partial}{\partial r} \left(\frac{\partial w}{\partial r} \frac{\partial r}{\partial y}\right) = \frac{j}{8\lambda^2 D} \left[\frac{\partial^2}{\partial r^2} [\Pi(\lambda r)] \left(\frac{y-y_s}{r}\right) + \frac{\partial}{\partial r} [\Pi(\lambda r)] \left(\frac{-(y-y_s)}{r^2}\right) \right] \quad (\text{A.17})$$

$$\frac{\partial}{\partial r} \left(\frac{\partial w}{\partial r} \frac{\partial r}{\partial y}\right) \frac{\partial r}{\partial y} = \frac{j}{8\lambda^2 D} \left[\frac{\partial^2}{\partial r^2} [\Pi(\lambda r)] \left(\frac{y-y_s}{r}\right) + \frac{\partial}{\partial r} [\Pi(\lambda r)] \left(\frac{-(y-y_s)}{r^2}\right) \right] \left(\frac{y-y_s}{r}\right) \quad (\text{A.18})$$

or

$$\frac{\partial}{\partial r} \left(\frac{\partial w}{\partial r} \frac{\partial r}{\partial y}\right) \frac{\partial r}{\partial y} = \frac{j}{8\lambda^2 D} \left[\frac{\partial^2}{\partial r^2} [\Pi(\lambda r)] \left(\frac{(y-y_s)^2}{r^2}\right) - \frac{\partial}{\partial r} [\Pi(\lambda r)] \left(\frac{(y-y_s)^2}{r^3}\right) \right] \quad (\text{A.19})$$

It can be written

$$\frac{\partial w}{\partial r} \frac{\partial^2 r}{\partial y^2} = \frac{j}{8\lambda^2 D} \frac{\partial}{\partial r} [\Pi(\lambda r)] \left[\frac{1}{r} - \frac{(y-y_s)^2}{r^3} \right] \quad (\text{A.20})$$

Then:

$$\frac{\partial^2 w}{\partial y^2} = \frac{j}{8\lambda^2 D} \left\{ \left[\frac{\partial^2}{\partial r^2} [\Pi(\lambda r)] \left(\frac{(y-y_s)^2}{r^2}\right) + \frac{\partial}{\partial r} [\Pi(\lambda r)] \left(\frac{1}{r} - \frac{2(y-y_s)^2}{r^3}\right) \right] \right\} \quad (\text{A.21})$$

Similarly:

$$\frac{\partial^2 w}{\partial x^2} = \frac{j}{8\lambda^2 D} \left\{ \left[\frac{\partial^2}{\partial r^2} [\Pi(\lambda r)] \left(\frac{(x-x_s)^2}{r^2}\right) + \frac{\partial}{\partial r} [\Pi(\lambda r)] \left(\frac{1}{r} - \frac{2(x-x_s)^2}{r^3}\right) \right] \right\} \quad (\text{A.22})$$

Then:

$$M_y = \frac{j}{8\lambda^2 D} \left\{ \left[\frac{\partial^2}{\partial r^2} [\Pi(\lambda r)] \left(\frac{(y-y_s)^2}{r^2} \right) + \frac{\partial}{\partial r} [\Pi(\lambda r)] \left(\frac{1}{r} - \frac{2(y-y_s)^2}{r^3} \right) \right] \right. \\ \left. + v \left[\frac{\partial^2}{\partial r^2} [\Pi(\lambda r)] \left(\frac{(x-x_s)^2}{r^2} \right) + \frac{\partial}{\partial r} [\Pi(\lambda r)] \left(\frac{1}{r} - \frac{2(x-x_s)^2}{r^3} \right) \right] \right\} \quad (\text{A.23})$$

or:

$$M_y = \frac{j}{8\lambda^2 D} \left\{ \left[\left(\frac{1}{r} - \frac{2(y-y_s)^2}{r^3} \right) + v \left(\frac{1}{r} - \frac{2(x-x_s)^2}{r^3} \right) \right] \frac{\partial}{\partial r} [\Pi(\lambda r)] \right. \\ \left. + \left[\left(\frac{(y-y_s)^2}{r^2} \right) + v \left(\frac{(x-x_s)^2}{r^2} \right) \right] \frac{\partial^2}{\partial r^2} [\Pi(\lambda r)] \right\} \quad (\text{A.24})$$

For $y=0$ and $x_s=0$:

$$M_y = \frac{j}{8\lambda^2 D} \left\{ \left[\left(\frac{1}{r} - \frac{2y_s^2}{r^3} \right) + v \left(\frac{1}{r} - \frac{2x^2}{r^3} \right) \right] \frac{\partial}{\partial r} [\Pi(\lambda r)] + \right. \\ \left. \left[\frac{y_s^2}{r^2} + v \frac{x^2}{r^2} \right] \frac{\partial^2}{\partial r^2} [\Pi(\lambda r)] \right\} \quad (\text{A.25})$$

The shear force can be calculated as [10]:

$$Q_y = -D \frac{\partial}{\partial y} (\nabla^2 w) \quad (\text{A.26})$$

$$\nabla^2 w = \frac{\partial^2 w}{\partial x^2} + \frac{\partial^2 w}{\partial y^2} \quad (\text{A.27})$$

$$Q_y = -D \nabla^2 \left(\frac{\partial w}{\partial y} \right) = -D \nabla^2 \left(\frac{\partial w}{\partial r} \frac{\partial r}{\partial y} \right) \quad (\text{A.28})$$

$$Q_y = -D \nabla^2 \left\{ \frac{(y-y_s)}{r} \frac{\partial}{\partial r} \left[\frac{j}{8\lambda^2 D} \Pi(\lambda r) \right] \right\} \quad (\text{A.29})$$

For $y=0$:

$$Q_y = -D \nabla^2 \left\{ \frac{-y_s}{r} \frac{\partial}{\partial r} \left[\frac{j}{8\lambda^2 D} \Pi(\lambda r) \right] \right\} \quad (\text{A.30})$$

$$Q_y = \frac{j y_s}{8\lambda^2} \nabla^2 \left\{ \frac{1}{r} \frac{\partial}{\partial r} [\Pi(\lambda r)] \right\} \quad (\text{A.31})$$